Comparison of Maximum-Likelihood List-Mode Reconstruction Algorithms in PET

Ralph Brinks, Colas Schretter, Carsten Meyer

Abstract— **In this work we compare images obtained from different list-mode reconstruction algorithms for PET data. Our analysis is based on list-mode data generated from a Geant4 simulation of the Jaszczak phantom. The first issue addressed is the influence of the raytracer used during reconstruction on the quality of the resulting images. We find that the Wu anti-aliased raytracer leads to better images than the Siddon algorithm at the expense of higher computational effort. The second question concerns a comparison of various modifications of the OSEM list-mode reconstruction algorithm. Here the convergent variant COSEM yields slightly better results at costs of much higher computational effort. However, the newer Enhanced COSEM does not need that effort to produce a similar image.**

Index Terms— **Positron-Emission-Tomography, PET, List-Mode Reconstruction, Maximum-Likelihood Estimation, Ordered Subset Expectation Maximization, Raytracer, Jaszczak Phantom**

I. Introduction

LIST-MODE acquisitions of positron emission tomography (PET) studies have entered clinical routine for various reasons. Maybe the most important one is that a list-mode acquisition can canonically keep the full spatial and temporal resolution of the PET measurement. Accordingly, list-mode (LM) reconstruction algorithms gain increasing attention. For clinical use it has to be assured that the reconstruction algorithms and the corresponding parameters are chosen properly to obtain an optimal image.

The objective of this work is to compare the performance and the results of a set of iterative LM reconstruction algorithms based on the maximum likelihood approach. The first part of our work deals with the influence of the raytracer of the reconstruction algorithm. We compare the common Siddon raytracer [1] with a raytracer known from computer graphics, the Wu anti-aliased raytracer [2]. In the second part of our work we compare recent variants of the ordered subset expectation maximization (OSEM) algorithm.

II. Methods

A. Experimental setup

Our analysis is based on list-mode data generated from a Geant4, [3], simulation of the Jaszczak hot rod phantom in air (see Fig. 1). The isotope used in the simulation was F-18, yielding 20 million true coincidences. To exclude secondary physical effects, scattered events were rejected and were not stored during the simulation. Then, the reconstruction algorithms were applied with a high number of iterations (up to 100), and after each (sub-) iteration the actual reconstructed image was dumped. Plotting the square root of the sum of the squared voxel differences between each image and the original emission image, i.e. the ℓ_2-norm of the error image, versus the corresponding (sub-)iteration number, we get a hook-shaped curve as shown in Fig. 2. The image belonging to the minimum of this curve is the best obtainable image in terms of the ℓ_2-norm. We call this image ℓ_2-optimal or just optimal.

R. Brinks and C. Meyer are with Philips Research Laboratories Europe, Aachen, Germany. C. Schretter is at leave of Université Libre de Bruxelles, Brussels, Belgium.

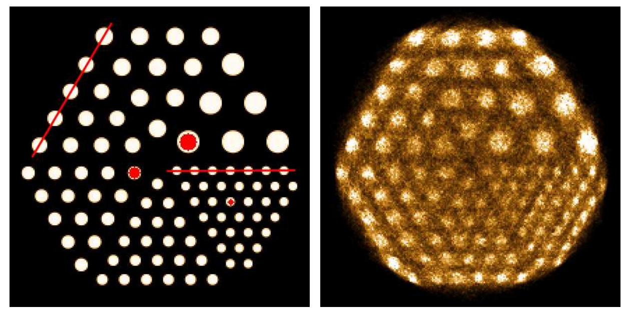

(a) (b)

Fig. 1. Jaszczak hot rod phantom in air (a) and the central slice of the reconstructed image (b). The inserted discs and lines mark respectively regions of interest (ROIs) and profiles used in our quantitative analysis. The ROIs are labeled from big to small with letters A, B and C. The horizontal line is referred as line A, the other as line B.

B. Image comparison

We compare the different reconstruction algorithms in terms of their optimal image (defined above). This optimal image is then examined further by an analysis of three different regions of interest (ROIs) and two line profiles as indicated in Fig. 1 (a). The central slice of the best image of the COSEM algorithm is shown in Fig. 1 (b). All images have $256 \times 256 \times 180$ cubic voxels of side length 1 mm.

For the ROIs the mean value $\bar{x}$ and the empirical standard deviation s_{n-1} are calculated. For the line profiles the mean ℓ_2-error (compared to the original image) are calculated. To summarize, we assess the quality of the reconstructed (optimal) image in terms of (i) the mean $\bar{x}$ and standard deviation s_{n-1} of the three different ROIs A, B and C shown in Fig. 1, (ii) the mean ℓ_2-error on the two lines A and B (Fig. 1), and (iii) the total ℓ_2-error.

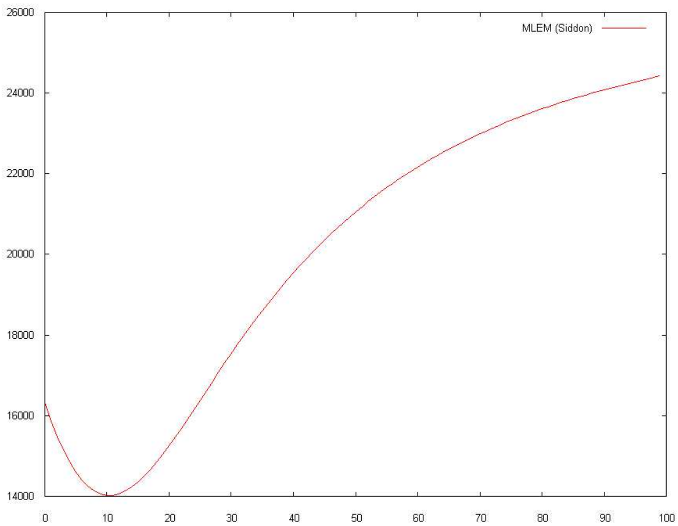

Fig. 2. ℓ_2-norm of the error image, versus iteration number of the MLEM reconstruction method.

C. Raytracer

The core of every LM reconstruction is the raytracer that processes the lines-of-responses (LORs). The raytracer is crucial for the image quality and the total computation time. We implemented both the Siddon raytracer and the Wu anti-aliased raytracer in a maximum likelihood expectation maximization (MLEM) algorithm and in the OSEM algorithm.

The classical Siddon raytracer [1] computes line integrals through a discrete grid of voxels by a weighted sum of values of every voxel in intersection with the line of response. The weight associated to a given voxel is proportional to the length of the line segment, clipped by the boundary planes of the voxel.

In order to model the finite resolution of PET systems, list-mode reconstruction algorithms could benefit from a volumetric raytracing procedure that approximates tubes of responses. For that purpose, the Wu anti-aliased line [2] technique, which is well known in the computer graphics community, has been adapted to three-dimensional images.

In the Wu raytracer, the weight associated to a given voxel is proportional to a fast approximation of the volume of intersection between a rectangular tube profile and the voxel. Fig. 3 shows graphically the difference between the line and tube of response models. The volumetric Wu method affects more voxels for a specific LOR than the Siddon technique.

D. OSEM variants

In the second part of our work, we compare several variants of the OSEM algorithm: the original OSEM, which in the general case is known not to be convergent, and two convergent extensions of OSEM, the so called complete data OSEM (COSEM, [4]) and the enhanced COSEM (ECOSEM, [5]).

The COSEM algorithm is derived from OSEM. OSEM computes a new image estimate by considering only a subset of the data. Instead of replacing the current image estimate by the newest one, the images are summed together in COSEM. When a subset is considered again with further iterations through the dataset, the previous image contribution that was computed with the classical OSEM procedure is also removed from the accumulation. For each subset, the previous image contribution is replaced by a fresh estimate. COSEM is therefore an additive algorithm and needs to retain the previous image contribution for every subset.

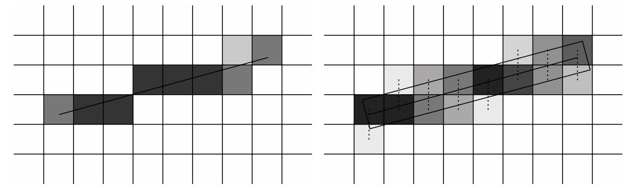

(a) (b)

Fig. 3. Siddon (a) and Wu (b) raytracing in an array of pixels. The tones of black are proportional to the lengths of the intersection between the line and pixels for Siddon and are proportional to an approximation of the intersection areas between the strip and pixels for Wu. The dotted segments link the centers of the two pixels, closest to the central line of the strip in (b).

The rationale behind the convergent property of COSEM method is that since the current image estimate sums up contributions from every subset, the limit-cycle behaviour of OSEM is avoided. However, the convergence can be slow at early iterations since the blurred preliminary image estimates are kept in the accumulation until the next iteration. Note that increasing the number of subsets does not alleviate this problem.

A hybrid reconstruction algorithm has been proposed to combine the early estimates of OSEM with the convergent behaviour of COSEM. The ECOSEM technique weights the contributions of both algorithms by a parameter to be set between one and zero. Rahmim et al., [6], suggest to use binary values for this parameter. With a binary schedule, the ECOSEM method is equivalent to applying OSEM at early sub-iterations, then switching to COSEM to polish the image estimate. Here, we compare the OSEM variants by calculating the performance measures addressed in section II-B.

III. Results

If we compare the ℓ_2-optimal Wu images with the optimal Siddon images by a Fisher sign test, we find that in both algorithms, MLEM and OSEM (here and in the following with 16 subsets), the images differ highly significantly ($\alpha = 0.001$). The optimal Wu raytraced images yield a better image quality in terms of the ℓ_2-norm of the error image, the mean in the ROIs and also in the ℓ_2-difference to the original image on the line profiles. A typical line profile is shown in Fig. 4.

The quantitative comparison of the raytracers and the reconstruction algorithms for the ℓ_2-optimal images are summarized in Table I. The relative time refers to the effort to reach the optimal image and is measured in units for one complete pass through the data (1 iteration) with the Siddon MLEM. The ROIs are labeled from big to small with letters A, B and C. The horizontal line is referred as line A, the other as line B, cf. Fig. 1 (a). Note that the true ROI mean in the original image is

TABLE I

STATISTICS OF ROIS AND LINE PROFILES ANALYSES. FOR A DEFINITION OF ROIS A, B AND C AND LINES A AND B SEE FIG. 1. THE RELATIVE TIME IS MEASURED IN UNITS FOR ONE COMPLETE PASS THROUGH THE DATA (1 ITERATION) WITH THE SIDDON MLEM.

Algorithm	Relative Time	ROI A		ROI B		ROI C		Mean ℓ_2-error on Line A	Mean ℓ_2-error on Line B	Total ℓ_2-error	# iter.
		$\bar{x}$	s_{n-1}	$\bar{x}$	s_{n-1}	$\bar{x}$	s_{n-1}				
MLEM Sid.	12	8.04	2.58	7.21	2.39	7.19	2.68	0.83	0.61	14002.23	12
MLEM Wu	27.16	8.57	2.63	7.72	2.40	8.25	3.14	0.77	0.62	13533.82	14
OSEM Sid.	0.75	8.13	3.00	7.43	2.69	7.18	3.13	0.81	0.66	14479.83	0.75
OSEM Wu	1.94	9.13	3.19	8.32	2.97	8.93	3.80	0.76	0.64	13672.41	1
COSEM Wu	8.12	8.40	2.62	7.59	2.38	8.21	3.18	0.77	0.63	13490.19	4
ECOSEM Wu	2.11	7.14	1.54	6.42	1.38	6.95	1.84	0.82	0.63	14026.11	1

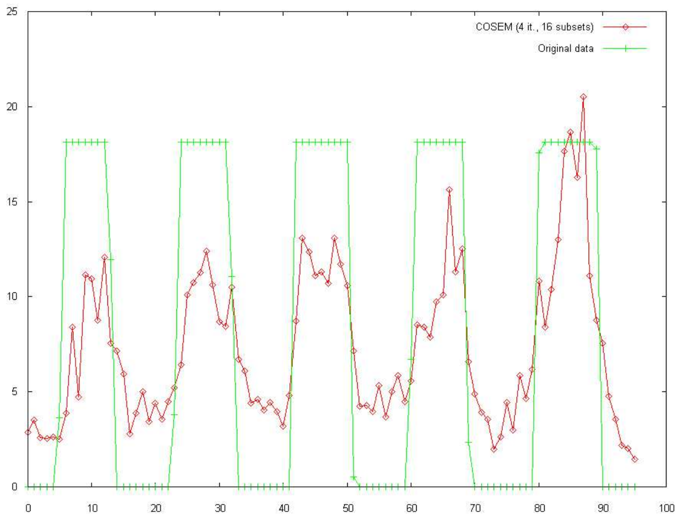

Fig. 4. Line profile (line B) after four iterations of the COSEM method and using 16 subsets.

18. With regard to the ROI values in the reconstructed images it can be stated that the ℓ_2-optimal images are far away from the true emission values.

The results show that in the MLEM and the OSEM cases, the Wu raytracer leads to the best results (at slightly increased noise). However, the Wu raytracer takes more than double the computational effort to reach the ℓ_2-optimal image. Surprisingly, the Siddon variant of OSEM yields the optimal image after 12 processed subsets, i.e. after 0.75 iterations.

For the comparison of the OSEM variants the Wu method is explored further. The OSEM algorithm took only one complete pass through the list-mode data to obtain the ℓ_2-optimal image. The COSEM needed four (!) complete passes, the ECOSEM one pass. This implies that COSEM needs 4.2 times longer than OSEM, ECOSEM only 1.1 times longer. The COSEM optimal image in terms of the ℓ_2-norm of the error image has been the best reconstructed image, which however is not the case for the ROI means. There the simple OSEM was best of all with the price of increased noise.

IV. CONCLUSION

In this work we analyzed different list-mode reconstruction algorithms of PET data obtained from a Geant4 simulation of the Jaszczak phantom. The first investigated issue was the influence of the raytracer used during reconstruction for the quality of the resulting images. We find that the Wu anti-aliased raytracer leads to better images than the Siddon algorithm, but needs more computational effort. There is an ongoing effort to accelerate the Wu algorithm. The second question addressed a performance comparison of several variants of the OSEM list-mode reconstruction algorithm. Here the convergent variant COSEM yields slightly better results at costs of much higher computational effort. However, the newer Enhanced COSEM does not need that effort to produce a similar image.

ACKNOWLEDGMENT

The authors would like to thank Michel Defrise from the Université Libre de Bruxelles for his insightful help and discussions.

REFERENCES

[1] R. Siddon "Fast Calculation of the Exact Radiological Path Length for a Three-dimensional CT Array" *IEEE Trans. Med. Phys.*, 12, pp. 252-7, 1985.

[2] X. Wu, "An Efficient Anti-aliasing Technique", *ACM Comp. Graph.*, 4 (25), pp. 143-52, 1991.

[3] J. Allison et. al. "Geant4 Developments and Applications" *IEEE Trans. Nucl. Sci.*, 53 (1), pp. 270-8, 2006

[4] I. T. Hsiao, A. Rangaraja, G. Gindi "A Probably Convergent OS-EM Like Reconstruction Algorithm for Emission Tomography" *Conf. Rec. SPIE Med. Imag.*, 4684, pp. 10-19, 2002

[5] I. T. Hsiao, A. Rangaraja, P. Khurd, G. Gindi "An Accelerated Convergent Ordered Subsets Algorithm for Emission Tomography" *Phys. Med. Bio.*, 49 (11), pp. 2145-56, 2004

[6] A. Rahmim, J.-C. Cheng, S. Blinder, M.-L. Camborde, and V. Sossi, "Statistical list-mode image reconstruction for the high resolution research tomograph," *Phys. Med. Bio.*, 49, pp. 4239-4258, 2004.